

Investigation on Transient Thermal Responses on 316L Austenitic Stainless Steel and Low Carbon Ferritic Steel Welding Using Pulsed Nd: YAG Laser

Kumar KS^{*1,2}

¹University of Madras, Chennai, Tamil Nadu, India

²P.T.Lee Chengalvaraya Naicker College of Engineering and Technology, Kanchipuram, Tamil Nadu, India

Abstract

Dissimilar welding of 316L stainless steel-low carbon ferritic steel joints made using pulsed Nd: YAG laser beam. The laser spot symmetrically focused on the butt joint and offset-*ted* by 2 μm to stainless steel to obtain the good quality of dissimilar weld. A three dimensional finite element based model developed using comsol code to simulate welding process for these two different laser spot positions. Thermal profile, isothermal surface, and deformation of the dissimilar joints simulated to investigate the temperature distribution across the butt joints. The temperature distribution estimated across the dissimilar joint analytically. The estimated and predicted results exposed the bead width and heat affected zone in dissimilar joints. These results were compared with experiment found that has very close association with each other.

Keywords: Pulsed laser welding; Austenitic stainless steel; Low carbon ferritic steel; Temperature distribution; Isothermal surface; Deformation

Introduction

Welding of different combinations of materials joints in accordance with change in working/operating temperature is on strong demand in the industry due to both technical and economic reasons [1]. However, many problems incurred with dissimilar joints such as selection of filler metal, different thermophysical and mechanical properties; therefore, the selection of proper welding variable is very important [2]. In most of the power plants, dissimilar welds joints are employed in many circumstances, one of those is to connect the heat exchanger to external pipe systems at the tailor ends. The combinations of 316L austenitic stainless steel and low carbon ferritic steel being used for these circumstances since it's possess a good combination of mechanical properties, formability and weldability.

Solid State Methods in Dissimilar Welding

Several joining processes used for joining of dissimilar materials such as explosion welding, pressure welding, friction welding, and soldering and brazing. For example, Aluminium alloy sheets were lap joined to galvanized steel sheets by gas tungsten arc welding (GTAW) with different Al filler wires, found the intermetallic compound (IMC) layer decreased and the tensile strength of the joint increased with the increase of Si content in the weld [3]. Micro-duplex stainless steel (MDSS) and titanium alloy (TiA) joined by atomic diffusion bond with 150 μm thick nickel alloy (NiA) interlayer as filler material [4]. The friction welding of dissimilar joints of AISI 316L stainless steel and cp-titanium, the magnitude of tensile strength was observed below that of the titanium base material if preheating was not applied at the interface [5].

Importance of Fusion Welding in Dissimilar Joints

Nevertheless, materials joint continue to be highly engineered in terms of metallic and metallurgical continuity and microstructural integrity, hence, fusion welding processes will become more prominent. When we use traditional fusion welding methods, 316L stainless steel joints are required to minimize the quantity of ferrite in the welds to avoid property degradation during service. Similarly, joining of low carbon ferritic steels have been facing the problem with undergoing

rapid grain growth, which leads to brittle, heat affected zones in the fabricated product. To some extent electron beam welding also suggested as suitable welding tool for dissimilar welding in industry application owing to high welding speed and excellent mechanical properties as compared to GTAW and FRW, but it is possible only at vacuum [2].

Brief History of Laser in Dissimilar Welding

Laser welding is the only alternate among fusion welding, addressing these issues and is used extensively to produce weld with its numerous advantages over conventional welding methods, for example, pulsed Nd: YAG laser welding of 321 stainless steel and 630 (17-4 pH) precipitations hardened stainless steel achieved very fine cellular and dendritic structures in the weld zone [6]. Pure niobium plate to the titanium alloy Ti-6Al-4V sheet using a pulsed Nd: YAG laser, no intermetallic hard phases were formed in the weld metal. Small islands of phases rich in Ti and Nb only identified in the fusion zone [7]. A combined laser welding and pre-and-post weld treatment technique used to overcome the crack formation in ferritic and martensitic stainless steel joints. Laser welding of AISI 420 martensitic stainless steel and kovar joints achieved, found no cracks in the weld [1]. An Al-Li based alloy joints made autogenously using Nd: YAG laser welding and find the decrease in the in quantity of δ' precipitates in the fusion zone [8]. Laser spot welds between low carbon and austenitic stainless steel lap joint had shown an asymmetric shape in fusion zone because of the different laser beam absorption and the thermal conductivity of the base metals [9]. Laser welding of various combinations of advanced high strength steels were presented in, revealed the high quality of the

***Corresponding author:** Kumar KS, University of Madras, Chennai, Tamil Nadu, India, Tel: 04425399422; E-mail: lectsuresh25@gmail.com

Received August 10, 2015; **Accepted** August 17, 2015; **Published** August 27, 2015

Citation: Kumar KS (2015) Investigation on Transient Thermal Responses on 316L Austenitic Stainless Steel and Low Carbon Ferritic Steel Welding Using Pulsed Nd: YAG Laser. J Material Sci Eng 4: 197. doi:10.4172/2169-0022.1000197

Copyright: © 2015 Kumar KS. This is an open-access article distributed under the terms of the Creative Commons Attribution License, which permits unrestricted use, distribution, and reproduction in any medium, provided the original author and source are credited.

weld joints [10]. Therefore, Nd: YAG pulsed laser welding expected to be the method of choice because it allows more precise heat control and reduces the width of heat-affected zone (HAZ), residual stress, and presence of discontinuities compared with other processes.

This article to describe the method of dissimilar welding of 316L austenitic stainless steel and low carbon ferritic steel sheets using pulsed Nd: YAG laser welding without filler material. An attempt made to achieve the symmetric fusion zone across the dissimilar weld joint. The transient thermal responses across the joint were estimated and computed are compared with experimental results.

Experimental Materials and Methods

Pair of 316L austenitic stainless steel and low carbon ferritic steel sheets having dimensions of 150 mm (Length) × 50 mm (Width) × 2 mm (Thickness) with smooth faces that is feasible for butt joint welding. The chemical compositions are given in Table 1. A systematic Nd: YAG laser beam with wavelength of 1.064 μm has delivered through 600 μm diameter silica core step index type optical fiber cable. The laser beam focused vertically on the surface at the focal distance of 200 mm with focused waist diameter of 451 μm for pulse duration 12 mS. The Nd: YAG laser source attached with highly précised CNC machine for accurate alignment at welding velocity fixed as 180 mm/sec. High purity of Argon (Ar) used as shielding gas, supplied at the flow rate 20l/min at the upper and lower faces of the plates at an angle 45° and the nozzle placed behind the laser beam. The schematic of the welding process and their operating parameters are given in Figure 1 and Table 2 respectively. The polished weld joints etched in 10% oxalic acid for stainless steel side and Nital for low carbon steel side to expose the features of the weld joint. A three dimensional finite element based modeling developed using comsol code to simulate the welding process. The laser pulses modeled as Hermit-Gaussian pulse, a volumetric heat source that spatially distributed in Transverse Electro Magnetic (TEM₀₀) mode. The micrographs taken at the range of magnification 500 μm to investigate the evolved weld pool at the butt joint interfaces using analysis software with PC controlled Optical Microscope. The ambient temperature was 293 K.

Results and Discussion

The laser spot was usually located symmetrically on the butt joint of specimens for the similar welding as shown in Figure 2a. However, dissimilar weld materials are showing vast differences in thermophysical properties, leads to uneven thermal profile on both sides. This may cause severe and undesirable changes in metallurgical and mechanical properties of the dissimilar weld joint. Form the materials considered for the experiment, low carbon ferritic steel is having higher thermal conductivity than the 316L stainless steel. Hence, it was decided to move the 451 μm dia focused laser spot by 2 μm towards 316L stainless steel side and located as shown in Figure 2b. Thus, heat input supplied to the low carbon steel reduced. The transient thermal responses predicted across both the point of irradiations during pulsed laser welding presented for the discussion.

Thermal profile of the dissimilar welds

Once the laser pulses start to irradiate on target fixed, heat generated by the phenomenon of light converting in to the heat energy. Figure 3 shows the comparison between the temperature distributions of dissimilar 316L austenitic stainless steel and low carbon ferritic steel sheet joints for two different focused laser spot positions as shown in Figure 2 during pulsed laser welding process. Figure 3a shows nearly an equal distribution of heat on both sides of the weld whereas we can

see some extension in heat distribution towards the low carbon ferritic steel side as shown in Figure 3b. This is because of higher thermal conductivity of low carbon ferritic steel than 316L stainless steel. It has controlled by giving reduced heat input to the low carbon side by way of minimizing laser interaction area on the surface. Hence, laser spot was offset-ted by 2 μm to 316L stainless steel side.

Isothermal surfaces of the dissimilar welds

It is important to distinguish the weld pool, heat affected zone and parent material regions around the dissimilar weld, because, volume of weld pool, heat affected zone playing vital role in quality of weld joint. Figure 4b shows the distribution of isothermal surfaces of dissimilar joint from laser spot location as shown in Figure 2b. The high melting, boiling point, densities, specific heat capacity and lower thermal conductivity of 316L stainless steel shows short range in heat distributions compared with other low carbon steel. The difference of material properties like thermal diffusivity in the solid and the liquid states also affects the penetration depth and weld pool shape. But, the laser is spotted as shown in Figure 2a, the contribution of convection relative to conduction in the overall heat transfer become more for 316L stainless steel and conduction in low carbon steel was restricted, thus, nearly an equal distribution of heat on both sides of the weld can be obtained as shown in Figure 4a.

Deformation of materials during the dissimilar welds

In the continuation of heat distribution onto the specimens,

Elements	C	Si	Mg	P	S	Ni	Cr	Mn	Fe
316L austenitic Stainless Steel	0.022	0.411	0.615	0.040	0.016	10.68	16.85	2.112	Balance
Low carbon ferritic steel	0.07	0.04	0.20	0.008	0.009	-	-	-	Balance

Table1: Chemical Composition of materials.

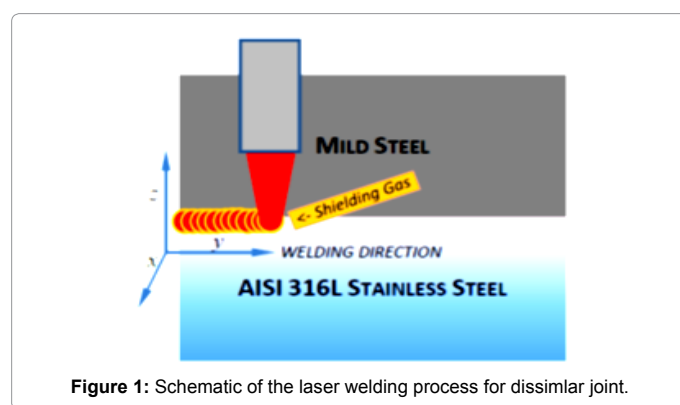


Figure 1: Schematic of the laser welding process for dissimilar joint.

Descriptions	Values
Average Peak Power	2100W
Pulse duration	12 mS
Frequency	15 Hz
Welding Velocity	180mm/min
Interaction Time	27 mS
Duty Cycle	18%
Pulse shape	Rectangular pulse
pulse energy	25.2J
Pulse over lapping	59%

Table 2: Operating parameters.

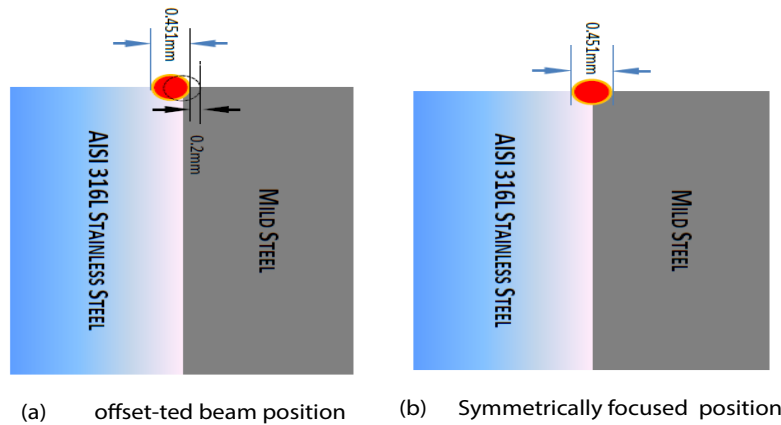


Figure 2: Schematic of the laser spot positions on the joint during welding process.

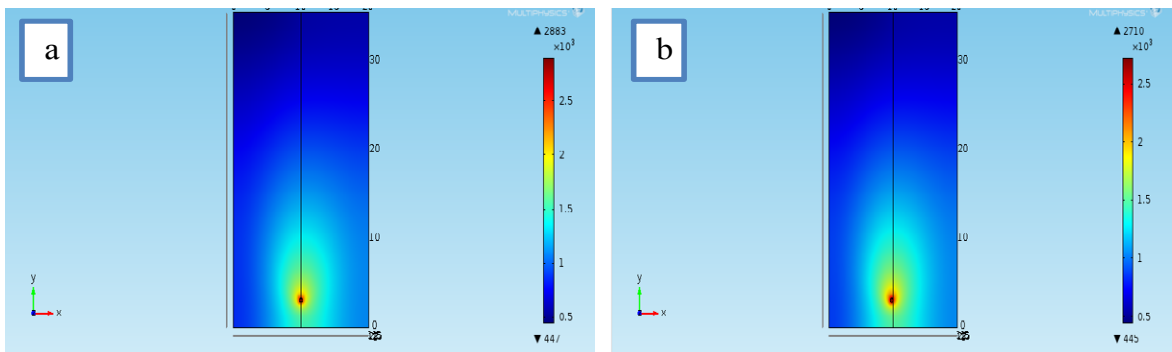


Figure 3: Comparison of temperature distributions for assumed laser spot positions on the joint during during pulsed laser welding process.

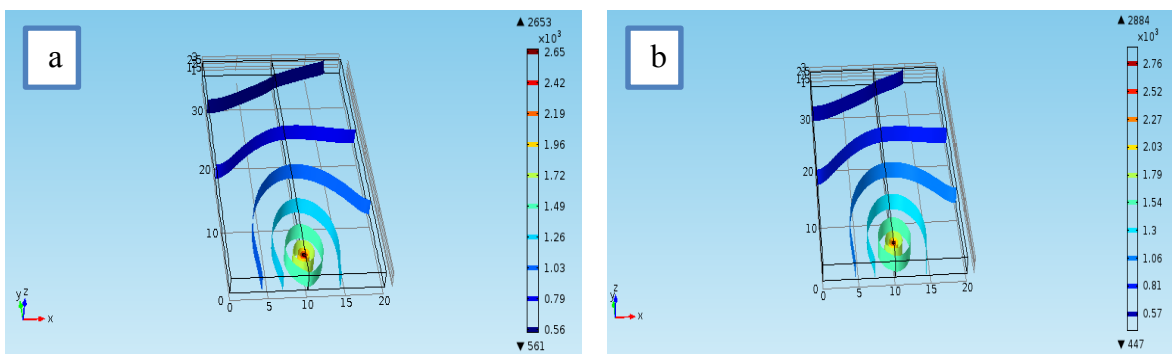


Figure 4: Comparison of isothermal surfaces for assumed laser spot positions on the joint during during pulsed laser welding process.

melting occurs via deformation where the laser being targeted. Again, due to lower melting point, low carbon steel was deformed more than the 316L stainless steel as shown in Figure 5b. The offset and the impingement angle of the laser beam are two key parameters for controlling the melt ratio of the dissimilar materials to avoid solidification cracking in the fusion zone and micro fissuring in the HAZ. So, the laser spot was offset- ted by 2 μm towards 316L stainless steel. This will help to give more heat input to 316L stainless steel and gets equal deformation compared to low carbon steel as shown in Figure 5a. Sound bead was produced over butt joints on 2 mm sheet at a 0.2 mm offset towards the 316L stainless steel with a 90° laser impingement angle.

Effect of temperature distribution when laser spot on weld-line

The temperature distributions are determined in various probe points from the centreline welding of 316L stainless steel-low carbon steel joint while laser spot symmetrically on it. Figure 6 illustrates the numerical results of the thermal analysis corresponding to the welding simulation process after a weld time of 10 s. The plotted results investigated by comparing probe points at equal distance on each side from the centreline weld. The focused laser spot diameter is 451 μm , hence, no direct irradiation takes place from the radial distance 1 to 5 mm. Therefore, the heat supplied via conduction and convection subsequently in radial distance. At 5 mm, the temperature increased

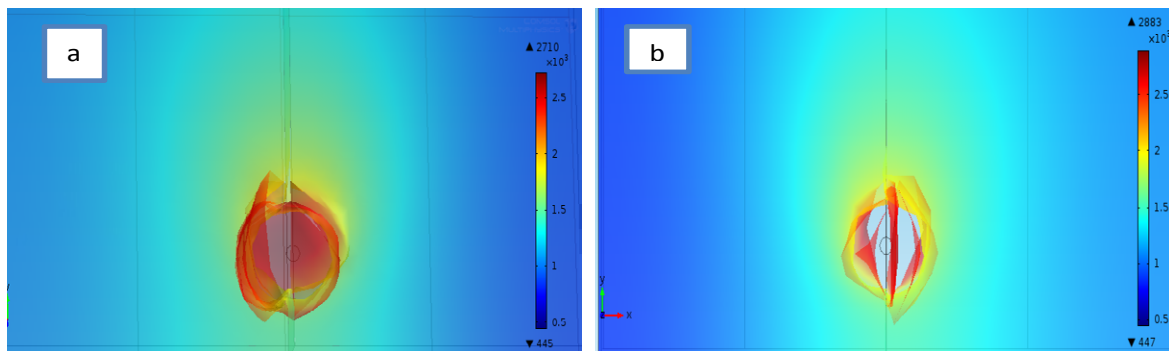
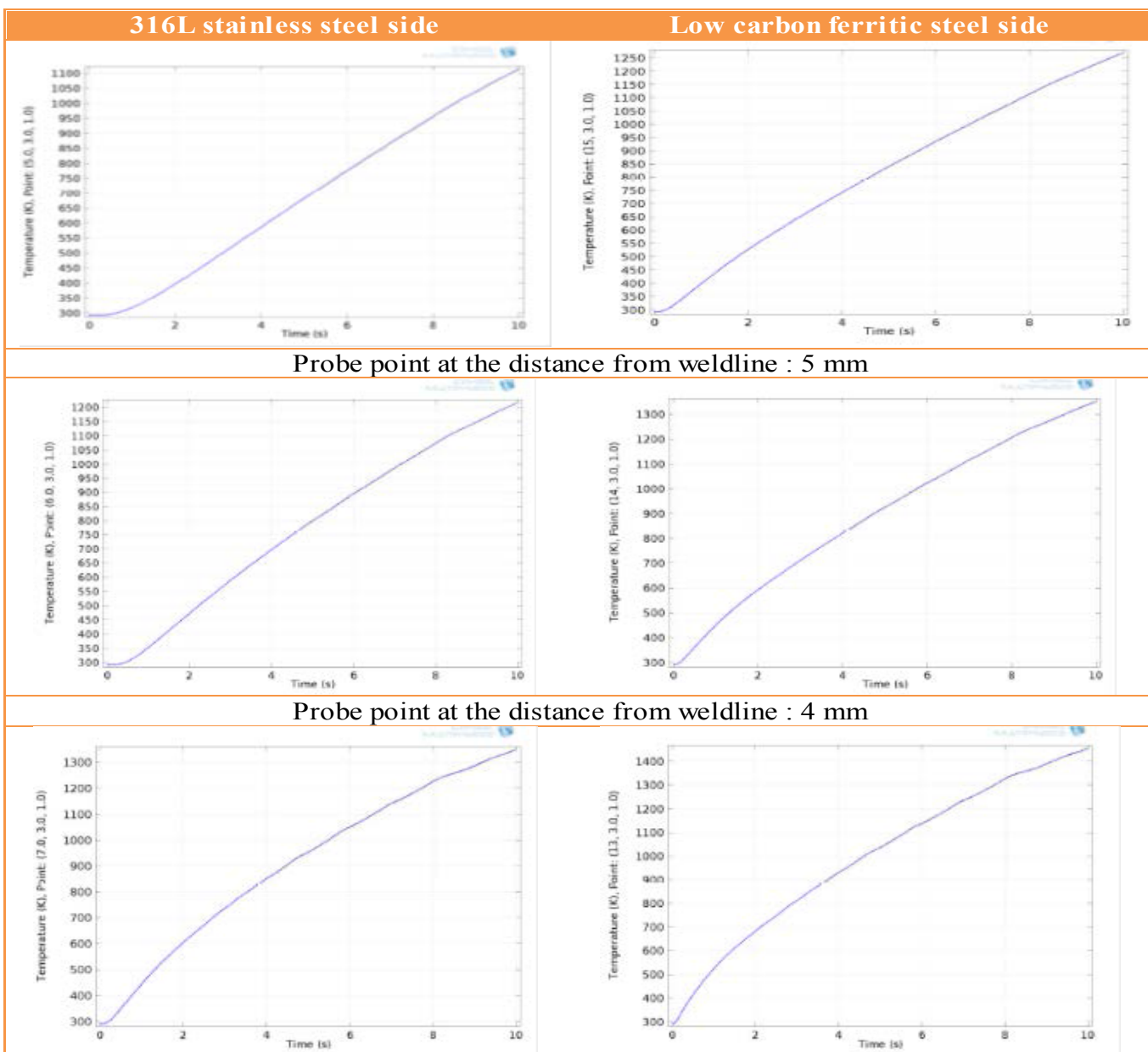


Figure 5: Deformation of the dissimilar joints for assumed laser spot positions on the joint during during pulsed laser welding process.



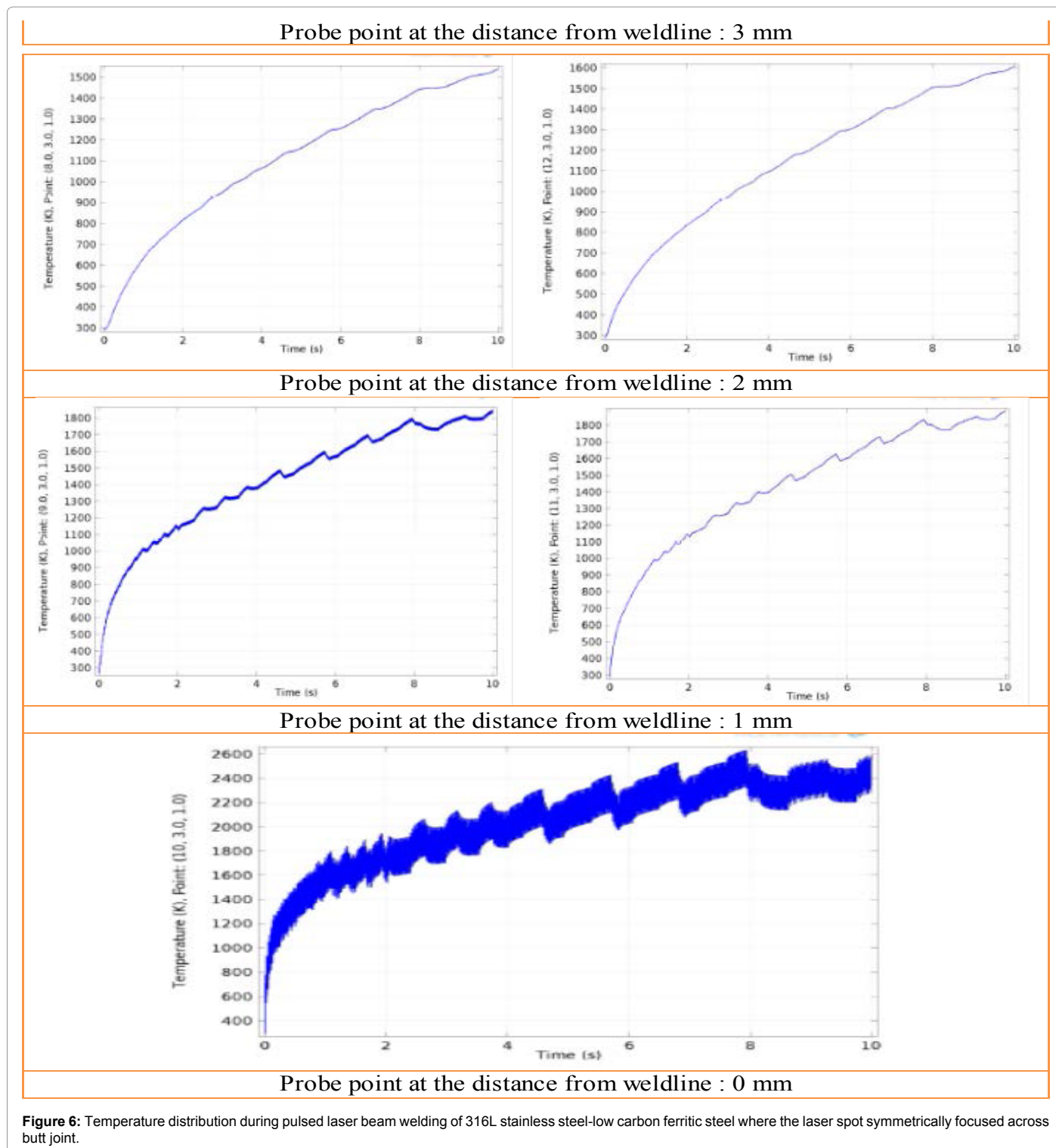


Figure 6: Temperature distribution during pulsed laser beam welding of 316L stainless steel-low carbon ferritic steel where the laser spot symmetrically focused across butt joint.

linearly with time. However, at 4 mm, there was a deviation observed in linearity of temperature curve, but no signs of fluctuation observed. At 3 mm, a clear non-linearity observed along with some signs of instabilities in the temperature curve. At 2 mm, temperature distribution observed in the form of parabolic curve with more oscillations. At 1mm, strong oscillations found in temperature curve on each side, at the same time, large thermal flux observed in 316L stainless steel, exhibiting high

resistance than the low carbon steel. It may be due to the phenomenon of destructive interference by overlapping of transient heat waves that produced by laser pulsation one after another. On the weldline where laser directly irradiates, clear and highest thermal flux was observed for every pulses. Thus, an asymmetry of the temperature field reveals the thermal profiles shown in Figures 3b, 4b and 5b due to different thermophysical properties of the base metals.

Effect of temperature distribution when laser spot offset to 316L stainless steel

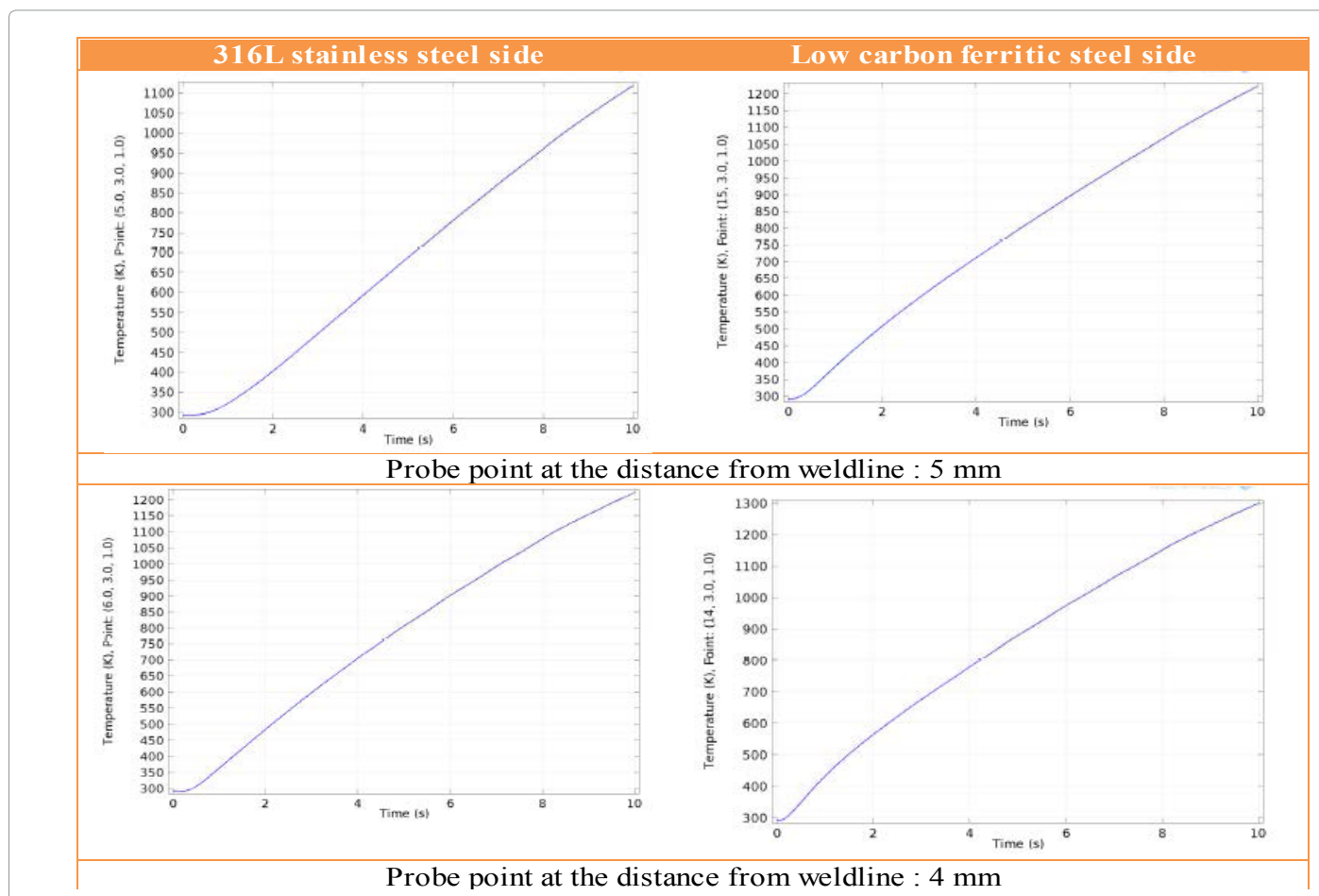
The temperature distributions are determined in various probe points from the centreline welding of 316 L stainless steel-low carbon steel joint while laser spot offset-ting by 2 μm towards 316L stainless steel as shown in Figure 2a. Figure 7 illustrates the numerical results of the thermal analysis corresponding to the welding simulation process after a weld time of 10 s. Nearly a similar way of temperature distribution observed from 2 mm to 5 mm as we discussed on Figure 6. However, the ranges of temperature predicted on each side are very close to each other. At 1 mm, it is very close to the point of laser irradiation, hence, strong oscillations and large thermal flux found on both sides. In this case, larger thermal flux observed in 316L stainless steel as that of the previous case. Similarly, an unusual but considerable thermal flux observed on low carbon steel than the previous case. This indicates convective flow of austenite to ferritic steel side, nearly an equal distribution of temperature observed on both the sides. Again, on the weldline, maximum thermal fluctuation observed for every pulse, but less than that of the previous case. This may be due to the strong convective heat transfer between the molten metals. Thus, an emphatic symmetry of the temperature field found that reveals the thermal profiles shown in Figures 3a, 4a and 5a possess an equal temperature distribution for producing dissimilar joint with good strength. The analytically estimated temperature distribution across dissimilar joint when the heat source offset by 2 μm to 316L stainless steel is given in Figure 8. The estimation is closely matching with predicted results in the heat-affected zone and slightly higher in the weldpool region.

Experimental investigation on the effect of laser spot positions

Temperature distribution during pulsed Nd: YAG laser beam welding for 316L stainless steel-low carbon ferritic steel were experimentally investigated as shown in Figures 9a and 9b where the laser spot symmetrically focused across butt joint. The pigmentations around the weld bead on both the sides reveal an emphatic asymmetry of the temperature field reveals the thermal profiles shown in Figures 3b, 4b and 5b due to different thermo-physical properties of the base metals. Similarly, Figures 10a and 10b shows the temperature distribution in 316L stainless steel-low carbon ferritic steel where the laser spot offset-ting by 2 μm to stainless steel, an emphatic symmetry of the temperature field that has very close association with the thermal profiles shown in Figures 3a, 4a and 5a. The estimated and predicted temperature distribution across the joint are closely matching with experimental results, found that the bead width lies between 2-3 mm, heat affected zone in 316 L stainless steel was found up to 8 mm and it was observed up to 10 mm in low carbon steel.

Conclusion

A three dimensional finite element based modeling developed using comsol code to simulate the welding process for those two different laser spot positions. Due to the asymmetrical distribution of temperature in sides of weld joint it has decided offset the laser spot position by 2 μm towards stainless steel across butt joint. Dissimilar welding of 316L stainless steel-low carbon ferritic steel weld joints



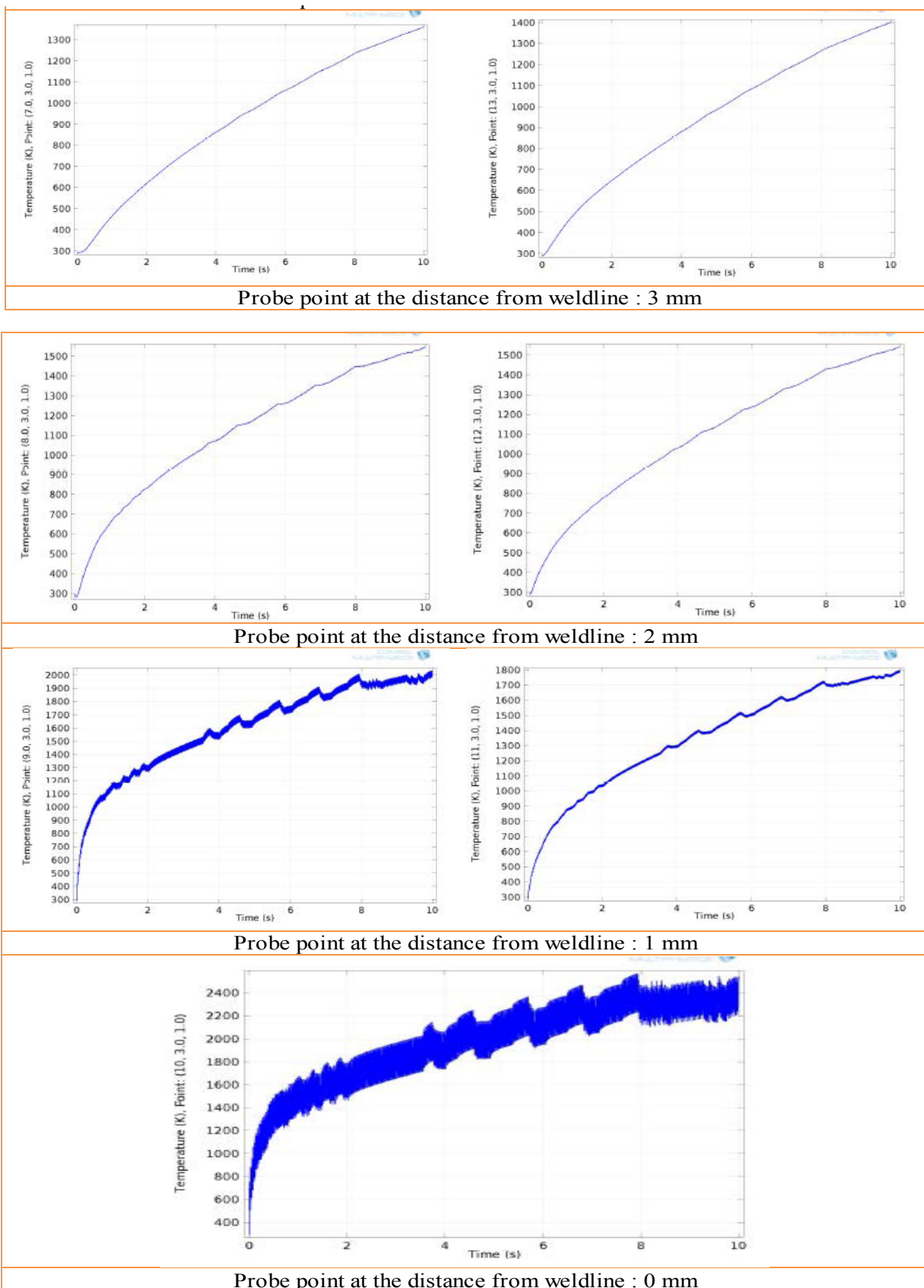


Figure 7: Illustrates the numerical results of the thermal analysis corresponding to the welding simulation process after a weld time of 10 s.

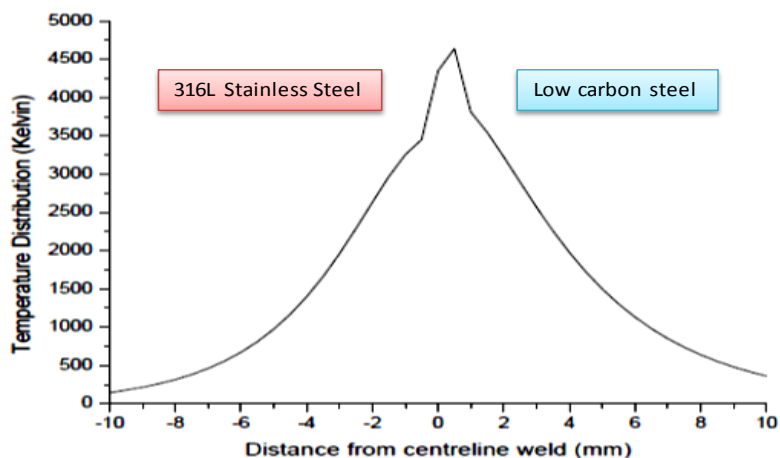


Figure 8: Analytically estimated temperature distribution across dissimilar weld when the heat source offset by 2 μm to 316L stainless steel.

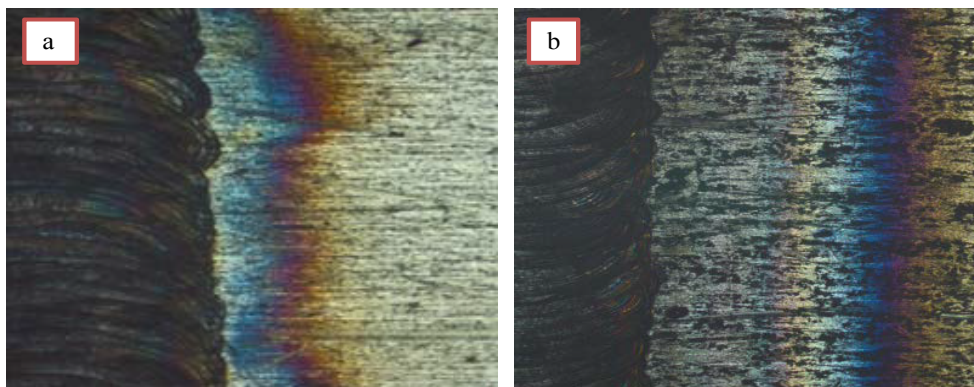


Figure 9: Temperature Distribution during pulsed Nd: YAG laser beam welding of 316L stainless steel-low carbon ferritic steel where the laser spot symmetrically focused across butt joint.

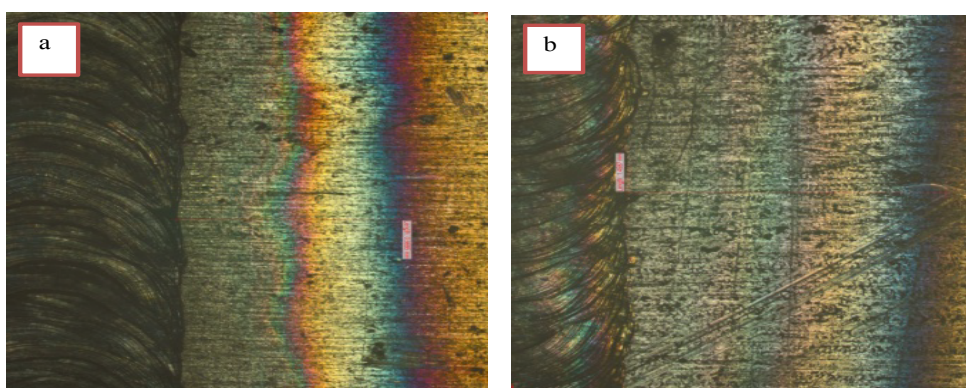


Figure 10: Temperature distribution during pulsed Nd: YAG laser beam welding of 316L stainless steel-low carbon ferritic steel where the laser spot offset-ted by 2 μm to stainless steel from symmetrically focused point across butt joint.

made using pulsed Nd: YAG laser beam at the symmetrically focused laser spot position. Thus, almost the evenly distributed temperature thermal profile and hence, acceptable weld bead achieved. The simulated thermal profile, isothermal surface and deformation of the dissimilar joints are investigated across the butt joints. The analytically and numerically predicted results are compared with the temperature distribution across the experimentally achieved dissimilar joint

that revealed very close association with each other. The decision of offsetting laser spot position for dissimilar welding joint will be very useful for different combinations.

Acknowledgements

The author wish to thank the authorities of "Indira Gandhi Centre for Atomic Research, Kalpakkam, Tamil Nadu, India for granting permission and providing facilities to carry out the experimental work.

References

1. Baghjari SH, Akbari Mousavi SAA (2013) Experimental investigation on dissimilar pulsed Nd: YAG laser welding of AISI 420 stainless steel to kovar alloy. *Materials and Design* 57: 128-134.
2. Arivazhagan N, Singh S, Prakash S, Reddy GM (2011) Investigation on AISI 304 austenitic stainless steel to AISI 4140 low alloy steel dissimilar joints by gas tungsten arc, electron beam and friction welding. *Materials and Design* 32: 3036-3050.
3. Dong HG, Hu W, Duan Y, Wang X, Dong C (2012) Dissimilar metal joining of aluminum alloy to galvanized steel with Al-Si, Al-Cu, Al-Si-Cu and Zn-Al filler wires. *Journal of Materials Processing Technology* 212: 458-464.
4. Kundu S, Sam S, Chatterjee S (2013) Interfacial reactions and strength properties in dissimilar titanium alloy/Ni alloy/micro duplex stainless steel diffusion bonded joints. *Materials Science & Engineering A* 560: 288-295.
5. Akbarimousavi SAA, Goharikia M (2011) Investigations on the mechanical properties and microstructure of dissimilar cp-titanium and AISI 316L austenitic stainless steel continuous friction welds. *Materials and Design* 32: 3066-3075.
6. Akbari Mousavi SAA, Sufizadeh AR (2009) Metallurgical investigations of pulsed Nd: YAG laser welding of AISI 321 and AISI 630 stainless steels. *Materials and Design* 30: 3150-3157.
7. Torkamany MJ, Malek Ghaini F, Poursalehi R (2014) Dissimilar pulsed Nd: YAG laser welding of pure niobium to Ti-6Al-4V. *Materials and Design* 53: 915-920.
8. Cuia L, Li X, He D, Chen L, Gong S (2012) Effect of Nd: YAG laser welding on microstructure and hardness of an Al-Li based alloy. *Material characterization* 71: 95-102.
9. Torkamany MJ, Sabbaghzadeh J, Hamed MJ (2012) Effect of laser welding mode on the microstructure and mechanical performance of dissimilar laser spot welds between low carbon and austenitic stainless steels. *Materials and Design* 34: 666-672.
10. Sharma RS, Molian P (2011) Weldability of advanced high strength steels using an Yb: YAG disk laser. *Journal of Materials Processing Technology* 211: 1888-1897.